

## Pad Adhesion Investigation and Layout Optimization

Xiaokang Huang, David Gonzalez, Duofeng Yue, Jinhong Yang\*, Jeremy Middleton\*, Van Tran, Bang Nguyen, Harold Isom

TriQuint Semiconductor, Inc., 500 W Renner Road, Richardson, TX 75080  
972-757-2845, [xiaokang.huang@tqs.com](mailto:xiaokang.huang@tqs.com)

\* TriQuint Semiconductor, Inc., 2300 NE Brookwood Parkway, Hillsboro, OR 97124

**Keywords:** Metal adhesion, Pad adhesion, Bump shear, Wire pull

### Abstract

Achieving proper bond pad strength is a challenge in semiconductor integrated circuit production. Low bump pad strength can cause both process yield issues at assembly and reliability failures in the application field. The optimization of bond pad strength is not only a function of wafer fabrication and bonding processes, but also the layout underneath the metal pads. In this paper, we investigated the bond pad strength as a function of metal underneath the bond pad metal and the impact of anchored dummy metal under the bond pads. A correlation between the bond pad strength and the amount of metal underneath the pad is established. Based on the experimental results, the bond pad strength and layout can be optimized to address product and process requirements.

### INTRODUCTION

The improvement of bond pad strength remains an area of ongoing investigation because inadequate bond pad strength can result in both process and assembly yield loss and/or reliability failures in field applications. Recently-concluded and on-going investigation includes layout optimization [1], novel structures [2] and, of course, in-line and assembly process improvements.

It was observed that the pad adhesion strength is different within a die as shown in Figure 1. The die circuitry layout is in the center of the area. There are 10 pads around the die edge. The adhesion strength of these pads is indicated by the size of the square markers outside the die. The small squares inside each marker indicate the variation of the pad adhesion strength at each pad location. Pad A is the strongest one with a very tight distribution and Pad B is the weakest one with a large variation. The difference between them is the structures under the pads. Pad A has a metal layer under the pad and anchored with a matrix of vias, while Pad B has a large amount of metal under the pad without via anchors. This means that the pad adhesion strength is not only process-dependent, but also sensitive to underlying design structures.

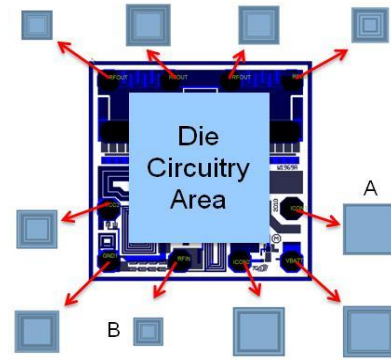


FIGURE 1 VARIATIONS OF PAD ADHESION STRENGTH WITHIN A DIE FOR DIFFERENT PADS AND ALSO WITHIN EACH PAD. THE SIZE OF THE SQUARE MARKERS OUTSIDE REPRESENTS THE ADHESION STRENGTH FOR EACH PAD

In this paper, we report the results of our investigation into bond pad strength as a function of metal beneath the pad metal itself and the impact of additional anchored dummy metal under the bond pads as obtained by bump shear tests. Based on the experimental results, the bond pad strength and layout can be optimized according to product and process requirements.

### PAD LAYOUT DESIGN FOR EXPERIMENTS

Figure 2(a) shows a typical bond pad structure. For better GaAs utilization and die size reduction requirements, both active components and passive structures are allowed, by Layout Design Rules (LDR), underneath the pads. These include transistors and diodes, metal connection lines, and resistors. For simplicity, only metal lines are shown under the pads in the drawing. Figure 2(b) is a similar pad structure with an additional metal line which is anchored to the pad through vias. The additional metal line is connected to the pad only for the purpose of enhancing the pad adhesion strength.

Pad structures are used for either wire connections in wire bond package or Cu bump connections in flip-chip package. The force in a wire bond is a pulling force perpendicular to the pad surface, while the force in Cu bump

bond is more a shearing force parallel to the pad surface. There are other factors in the wire pull test, such as wire thickness, wire strength, and pad surface condition, which affect the pad adhesion test results. Therefore, although data of both wire pull and bump shear tests were collected, only results from bump shear tests will be discussed below. The results and conclusions here can be applied to wire pull or wire bond package.

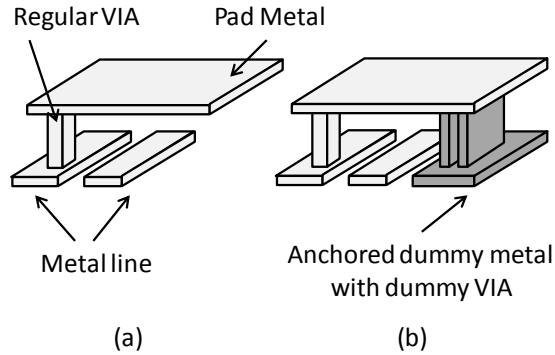


FIGURE 2 TYPICAL BOND PAD STRUCTURES CONNECTED TO A METAL LINE UNDERNEATH. (A) METAL LINES UNDER PAD METAL IN NORMAL CASES; (B) ADDITIONAL ANCHORED METAL STRUCTURE ADDED UNDER THE PAD METAL FOR MECHANICAL PAD STRENGTH IMPROVEMENT PURPOSE ONLY

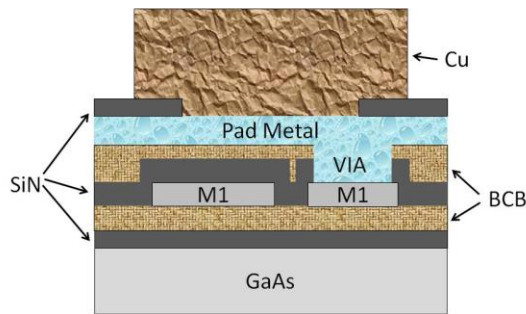


FIGURE 3 A DIAGRAM SHOWING A CU BUMP, A PAD METAL, AND STRUCTURES UNDERNEATH THE PAD.  $\text{Si}_3\text{N}_4/\text{M1}$  INTERFACE IS THE WEAKEST ONE DUE TO AU CHEMICAL INERT PROPERTY

Figure 3 gives the diagram of pad cross-section showing the different layers related to or affecting pad adhesion. For simplicity, there are only two layers of metal shown here, pad metal and metal 1 (M1). In our study, both metals are plated Au. The dielectric layers between metals and GaAs substrate are combination of  $\text{Si}_3\text{N}_4$  and bisbenzocyclobutene (BCB). There are six different interfaces which can impact the pad adhesion strength: Cu to Au metal, Au to BCB, BCB to  $\text{Si}_3\text{N}_4$ ,  $\text{Si}_3\text{N}_4$  to Au,  $\text{Si}_3\text{N}_4$  to GaAs substrate, and Au/VIA bond. Normally, dielectric films do not have strong adhesion to Au, because there are no chemical reactions to strengthen the bond and this bond is mainly mechanical in nature. The  $\text{Si}_3\text{N}_4$  and M1 Au interface is the focus of the pad adhesion improvement experiments discussed in this paper.

Different sizes and shapes of both anchored and non-anchored M1 are designed. The non-anchored M1 patterns are used to simulate the normal metal interconnect structures and the anchored M1 patterns are used for improving pad adhesion. The typical shapes of M1 are shown in Figure 4. For comparison, there are patterns with non-anchored M1 only and with additional anchored M1 in open areas where is without non-anchored M1. Patterns are paired as shown in Figure 4, (a) and (b), (c) and (d), (e) and (f), and (g) and (h). The patterns are only for showing the structures and they are not in scale. The shapes, sizes, and numbers of vias, which anchor M1 and bond pads, vary case by case.

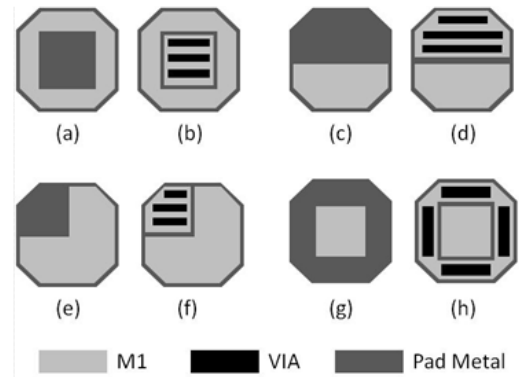


FIGURE 4 DIFFERENT LAYOUT STRUCTURES FOR PAD ADHESION STRENGTH EVALUATION WITH NON-ANCHORED M1 SIZE VARIATION AND ADDITIONAL ANCHORED M1 STRUCTURES

## EXPERIMENTS AND DISCUSSIONS

As mentioned earlier, bump shear test is used for the pad adhesion strength evaluation. The Cu bump shear machine is Nordson Dage 4000. The shear height is  $15\mu\text{m}$  from bottom of Cu bump. The shear speed is  $300\mu\text{m/s}$ . The tip is a flat end.

The typical images after bump shear are shown in Figure 5. The shear direction is upward as indicated in the figure. For convenience, the pad layouts are also shown in the figure paired with images. In all three cases, pad peeling starts from M1 Au surface as expected. This proves that the interface between  $\text{Si}_3\text{N}_4$  and Au is the weakest interface among the five interfaces in the pad structure shown in Figure 3. The surface layers in each case are determined with EDX measurement. In the case (a), there is no extra anchored M1, therefore BCB surface under pad metal exposed at the area without non-anchored M1. In the case (b), there is an area with additional anchored M1 to improve the pad strength. However, since the anchored M1 area is too small and the vias are not strong enough to hold both M1 and pad metal, these vias were cut off during the shear test. Therefore both M1 and via patterns can be seen in that area. In the case (c), the anchored M1 area is large and strong enough to hold both M1 and pad metal to each other,

therefore, pad peeling happens at the interface of M1 and BCB layer below it.

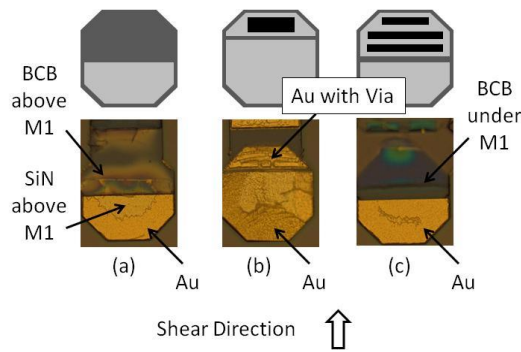


FIGURE 5 TYPICAL PAD IMAGES AFTER BUMP SHEAR. (A) A PAD WITH NON-ANCHORED M1 UNDERNEATH ONLY; (B) A PAD WITH LARGE NON-ANCHORED M1 AND ADDITIONAL SMALL ANCHORED M1; (C) A PAD WITH BOTH NON-ANCHORED M1 AND ADDITIONAL ANCHORED M1 UNDERNEATH

The correlations of the bump shear strength and the non-anchored amount of M1 area underneath the pad metal are shown in Figure 6. In Figure 6(a), the vertical axis is the minimum value of bump shear strength. The horizontal axis is the percentage of non-anchored M1 relative to the pad size. Gray boxes are from pads with non-anchored M1 under them only. Black boxes are from pads with both non-anchored M1 and anchored M1 underneath the pads.

There are three regions in Figure 6(a) and (b) denoted by the amount of non-anchored M1. In region (I), non-anchored M1 is in the range of 0 to 40% of the pad metal. In this region, the minimum bump shear strength is stable for both pads with non-anchored M1, and with additional anchored M1. Region (II), shows that increasing the amount of non-anchored M1 under the pad metal, the minimum values of the bump shear strength decrease for both types of pads. However, pads with non-anchored M1 have more low minimum values than pads with anchored M1. In the region (III), where the amount of non-anchored M1 is as large as 80 to 90% of pad size, there is little difference between non-anchored M1 and anchored M1 pads. Figure 6(b) shows the relationship between the standard variation in bump shear strength and anchored metal amount in the three regions previously discussed. As expected, the pads with additional anchored M1 have a tighter distribution than pads with only non-anchored M1 underneath. Therefore, additional anchored M1 under the pads helps improve the pad adhesion strength, especially by eliminating the lower points of the bump shear. In order to have consistent bump shear strength, the non-anchored M1 under pad metal should be kept smaller than 40%. If the non-anchored M1 size has to be larger than 40%, then additional anchored M1 should be added to where it can to strengthen the pads. The investigation shows that non-anchored M1 larger than 70% of pad size should be avoided.

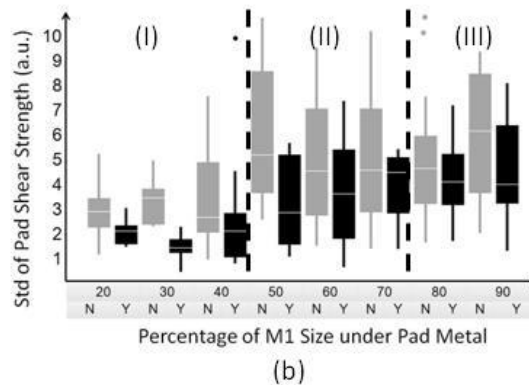
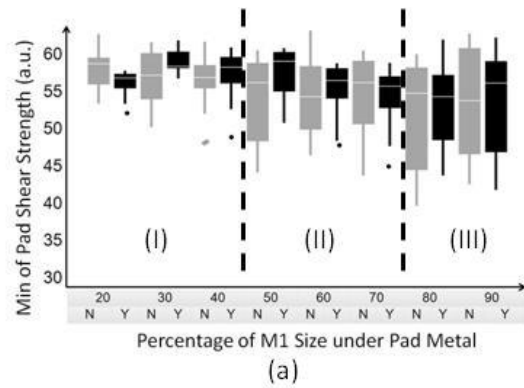


FIGURE 6 CORRELATIONS BETWEEN BUMP SHEAR STRENGTH AND NON-ANCHORED M1 UNDERNEATH PADS. (A) THE MINIMUM VALUE OF BUMP SHEAR STRENGTH AND (B) THE STANDARD VARIATION OF BUMP SHEAR STRENGTH. GRAY BOXES: PADS WITH NON-ANCHORED M1 ONLY; BLACK BOXES: PADS WITH ADDITIONAL ANCHORED M1

The data in Figure 6 is an overall summary of different shapes and sizes of M1 patterns and bump shear directions. The shear strength has a very strong dependence on both pattern shapes and shear directions. Figure 7 shows two types of layout patterns. Figure 7(a) is with only non-anchored M1 and (b) is with additional anchored M1. Both of them are sheared with two directions:  $0^\circ$  (upward) and  $180^\circ$  (downward). Figure 8 shows the shear strength as a function of non-anchored M1 size, shear direction, and whether there is an additional anchored M1 or not. It was observed that when the shearing starts from the non-anchored M1 side ( $0^\circ$  upward shearing), the weak interface of  $\text{Si}_3\text{N}_4$  and Au M1 is torn apart first. In this case, it does not matter much whether there is additional anchored M1 at the other end or not. However, when the shearing starts from the opposite side ( $180^\circ$ , downward shearing), the weak interface of  $\text{Si}_3\text{N}_4$  and Au M1 will not be affected by the shearing force immediately unless the non-anchored M1 size is large. As a result, a stronger M1 size dependence is seen in the  $180^\circ$  shearing direction and the pads with additional anchored M1 have a much tighter distribution and higher shear strength as expected.

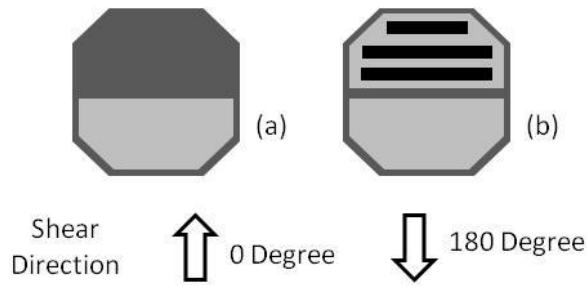


FIGURE 7 PATTERNS FOR INVESTIGATION OF SHEAR DIRECTION DEPENDENCE. (A) WITH NON-ANCHORED M1 ONLY; (B) WITH BOTH NON-ANCHORED M1 AND ADDITIONAL ANCHORED M1

However, since there can be shear forces from all directions, the application of this learning will need to be considered early in the design of the device and package itself. In some cases, the application will be straightforward; in other cases, compromises will need to be made.

### CONCLUSIONS

The impact of additional anchored M1 underneath pads on pad adhesion strength was experimentally investigated. The additional anchored M1 helps the pad adhesion by eliminating low strength points. Overall, reducing non-anchored M1 size has more impact on the pad adhesion strength. Keeping the amount of non-anchored M1 at or below 40% of the pad size results in more consistent pad strength. Our work demonstrated that optimization of pad shear strength may at times require an increase in die size. We believe there is an optimal point where technical and financial requirements can be balanced properly and achieved.

### ACKNOWLEDGMENTS

The authors would like to thank Peter Moon, Chi-hing Choi and Paul Miller for fruitful discussion. Thanks also go to Mary McAdams for layout modification, Robbie Skinner for bump shear data collection, and Wade Skelton and Timmy Ngo for wire pull sample preparation and data collection.

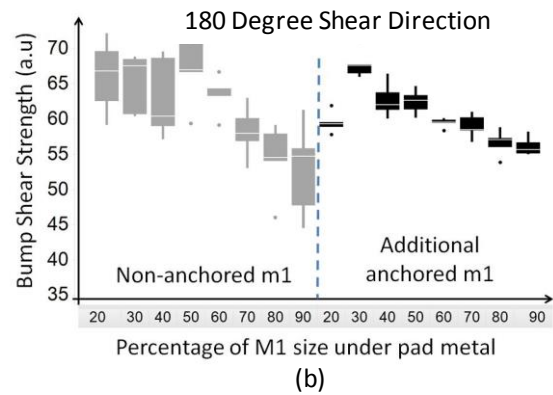
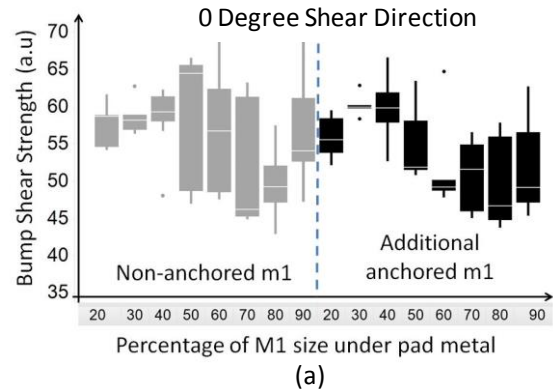


FIGURE 8 THE SHEAR STRENGTH AS A FUNCTION OF NON-ANCHORED M1 AND SHEAR DIRECTIONS. SHEAR DIRECTION: (A) 0 DEGREE AND (B) 180° AS DEFINED IN FIGURE 7.

### REFERENCES

- [1] Hunter, S., "Recent development work in IC bond pad structure and circuit under pad," Presentation to IMAPS Student Chapter, UI, September 2011.
- [2] C.-H. Yu and T.-I. Bao, "Bond pad structure having dummy plugs and/or patterns formed there around," US Patent 20100072632, March 2010.

### ACRONYMS

- LDR: Layout Design Rule
- BCB: bisbenzocyclobutene

